



Backdoor Attack and Defense in Federated Generative Adversarial Network-based Medical Image Synthesis

Ruinan Jin^a, Xiaoxiao Li^{b,1,*}

^aComputer Science Department, The University of British Columbia, BC, V6T 1Z4, Canada

^bElectrical and Computer Engineering Department, The University of British Columbia, BC, V6T 1Z4, Canada

ARTICLE INFO

Article history:

Keywords: Generative Adversarial Networks, Federated Learning, Backdoor Attack

ABSTRACT

Deep Learning-based image synthesis techniques have been applied in healthcare research for generating medical images to support open research and augment medical datasets. Training generative adversarial neural networks (GANs) usually require large amounts of training data. Federated learning (FL) provides a way of training a central model using distributed data while keeping raw data locally. However, given that the FL server cannot access the raw data, it is vulnerable to backdoor attacks, an adversarial by poisoning training data. Most backdoor attack strategies focus on classification models and centralized domains. *It is still an open question if the existing backdoor attacks can affect GAN training and, if so, how to defend against the attack in the FL setting.* In this work, we investigate the overlooked issue of backdoor attacks in federated GANs (FedGANs). The success of this attack is subsequently determined to be the result of some local discriminators overfitting the poisoned data and corrupting the local GAN equilibrium, which then further contaminates other clients when averaging the generator's parameters and yields high generator loss. Therefore, we proposed FedDetect, an efficient and effective way of defending against the backdoor attack in the FL setting, which allows the server to detect the client's adversarial behavior based on their losses and block the malicious clients. Our extensive experiments on two medical datasets with different modalities demonstrate the backdoor attack on FedGANs can result in synthetic images with low fidelity. After detecting and suppressing the detected malicious clients using the proposed defense strategy, we show that FedGANs can synthesize high-quality medical datasets (with labels) for data augmentation to improve classification models' performance.

© 2023 Elsevier B. V. All rights reserved.

1. Introduction

While deep learning has significantly impacted healthcare research, its impact has been undeniably slower and more limited in healthcare than in other application domains. A significant reason for this is the scarcity of patient data available to

the broader machine learning research community, largely owing to patient privacy concerns. Although healthcare providers, governments, and private industry are increasingly collecting large amounts and various types of patient data electronically that may be extremely valuable to scientists, they are generally unavailable to the broader research community due to patient privacy concerns. Furthermore, even if a researcher is able to obtain such data, ensuring proper data usage and protection is a lengthy process governed by stringent legal requirements. This

*Corresponding author: Xiaoxiao Li
e-mail: xiaoxiao.li@ece.ubc.ca (Xiaoxiao Li)

can significantly slow the pace of research and, as a result, the benefits of that research for patient care.

Synthetic datasets of high quality and realism can be used to accelerate methodological advancements in medicine (Dube and Gallagher, 2013; Buczak et al., 2010). While there are methods for generating medical data for electronic health records (Dube and Gallagher, 2013; Buczak et al., 2010), the study of medical image synthesis is more difficult as medical images are high-dimensional. With the growth of generative adversarial networks (GAN) (Goodfellow et al., 2014), high-dimensional image generation became possible. Particularly, conditional GAN (Mirza and Osindero, 2014) can generate images conditional on a given mode, e.g. constructing images based on their labels to synthesize labeled datasets. In the field of medical images synthesis, Teramoto et al. (2020) proposed a progressive growing conditional GAN to generate lung cancer images and concluded that synthetic images can assist deep convolution neural network training. Yu et al. (2021) recently used conditional GAN-generated pictures of aberrant cells in cervical cell classification to address the class imbalance issue. In addition, a comprehensive survey about the role of GAN-based argumentation in medical images can be found in Shorten and Khoshgoftaar (2019).

Like most deep learning (DL)-based tasks, limited data resources is always a challenge for GAN-based medical synthesis. In addition, large, diverse, and representative dataset is required to develop and refine best practices in evidence-based medicine. However, there is no single approach for generating synthetic data that is adaptive for all populations (Chen et al., 2021). Data collaboration between different medical institutions (of the heterogeneity of phenotypes in the gender, ethnicity, and geography of the individuals or patients, as well as in the healthcare systems, workflows, and equipment used) makes effects to build a robust model that can learn from diverse populations. But data sharing for data collection will cause data privacy problems which could be a risk of exposing patient information (Malin et al., 2013; Scherer et al., 2020). Federated learning (FL) (Konečný et al., 2016) is a privacy-preserving tool, which keeps data on each medical institute (clients) locally and exchanges model weights with the server to learn a global model collaboratively. As no data sharing is required, it is a popular research option in healthcare (Rieke et al., 2020; Usynin et al., 2022). Federated GAN (FedGAN) is then proposed to train GAN distributively for data synthesis Augenstein et al. (2019); Rasouli et al. (2020). *Its overall robustness against attacks is under explored.*

However, as an open system, FL is vulnerable to malicious participants and there are already studies deep dive into different kinds of attacks for classification models in federated scenarios, like gradient inversion attacks (Huang et al., 2021), poisoning and backdoor attacks (Bagdasaryan et al., 2020). In a backdoor attack with classification models, the attacker, such as a malicious client, adds a "trigger" signal to its training data and identifies any image with a "trigger" as other classes (Saha et al., 2020). A "trigger," such as a small patch with random noise, could lead a sample to be misclassified to another class. This kind of attack takes advantage of the classification model's

tendency to overfit the trigger rather than the actual image (Bagdasaryan et al., 2020). It is worth noting that numerous medical images naturally exhibit backdoor-like triggers and noisy labels, as depicted in Fig. 1, which enhances the significance of backdoor studies in the field of medical image analysis (Xue et al., 2022). Unfortunately, the server cannot directly detect the attacked images given the decentralized nature of FL, where the clients keep their private data locally. Recently, several studies found backdoor attached clients can cause a substantial drop in the classification performance in FL (Tolpegin et al., 2020; Sun et al., 2021). These facts inspire us to think about how backdoor attack affects generative models in FL.

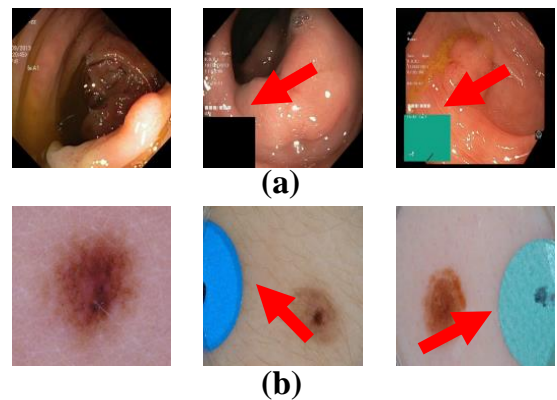


Fig. 1: Example medical images with backdoor-alike noisy patches from (a)KVASIR dataset (Pogorelov et al., 2017) (b) ISIC dataset (Codella et al., 2018)

In this work, we focus on backdoor attacks in the labeled medical image synthesis using conditional FedGAN. In our experiments, we employ two widely used medical datasets. First, we demonstrate the effect of adding different sizes and types of the trigger (e.g., a patch with different pattern and sizes ranging from 0.5 to 6.25 percent of the original image size) can significantly affect the fidelity of the generated images. Second, we propose an effective defense mechanism, FedDetect, to detect malicious client(s). We observe that the attacked discriminator tends to overfit, yielding inconsistent and different training loss patterns. Therefore, FedDetect performs outlier detection on clients' shared training loss in each iteration and red flags a client as malicious if it is detected as an outlier based on its record in multiple iterations. Our results first qualitatively compare the visualizations of the generative images of FedDetect and with the alternative defense strategies under backdoor attacks with different trigger sizes. Furthermore, with the FedGAN-assisted diagnostic as a signifier for FedGAN's role in the field of medicine, we quantitatively evaluate the effect of FedGAN-assisted data augmentation for DL training, the attack, and FedDetect. It shows that FedGAN-assisted data augmentation effectively improves the performance of DL training, while synthetic medical images generated from the attacked FedGANs corrupt their utility, leading to a poor medical utility value. FedDetect blocks such adversarial and builds up a Byzantine-Robust FedGAN (Fang et al., 2020).

Our contributions are summarized as follows:

- To the best of our knowledge, we are the first to examine the robustness of FedGAN, a promising pipeline for medical data synthesis, from the practical backdoor attack perspectives. Without loss of generality, we examine our proposed pipeline, attack, and defense on two public medical datasets.
- We propose a general pipeline of conditional FedGAN to generate labeled medical datasets. We extend backdoor attacks for classification models to generative models and reveal the vulnerability of conditional FedGAN training by backdoor attacks. We investigate the effect of different trigger sizes and types in the attacks.
- We propose an effective defense strategy FedDetect and compare it with the current practices to show its irreplaceable role in achieving robust FedGANs. We not only present qualitative results by examining the fidelity of the synthetic data, but also quantitatively evaluate their utility as data augmentation to assist diagnostic model training. We show the practical use and the innovation of FedDetect in the field of medical image synthesis.

A preliminary version of this work, Backdoor Attack is a Devil in Federated GAN-based Medical Image Synthesis (Jin and Li, 2022) has been presented in SASHIMI 2022. This paper extends the preliminary version by expanding the conditional FedGAN which generates synthetic medical images with labels so that synthetic images can serve for broader usage (such as data augmentation), examining the effect of various sizes and types of triggers with gray-scale and RGB medical datasets, performing quantitative analysis on the synthetic data, and assessing the utility of the synthetic medical images as data augmentation to assist training deep diagnostic models.

2. Preliminaries and Related Work

2.1. Conditional Generative Adversarial Networks

GAN was first been proposed in Goodfellow et al. (2014) as an unsupervised generative algorithm, where two deep neural networks, discriminator and generator are training against each other to optimize minmax objective function Eq. 1.

$$\min_G \max_D \mathbb{E}_{x \sim p_{\text{data}}(x)} [\log D(x)] + \mathbb{E}_{z \sim p_z(z)} [\log (1 - D(G(z)))], \quad (1)$$

where G and D are generator and discriminator, x is the training data, and z is a random noise vector sampled from a predefined distribution p_z . GAN has been used to generate medical image datasets for data augmentation and data sharing for open research as healthcare institutions are regulated to release their collected private data (Chen et al., 2022; Lin et al., 2022).

Later, Mirza and Osindero (2014) implemented the conditional GAN, turning GAN to be supervised learning algorithm, where both the discriminator and the generator take an extra auxiliary label so that GAN generates images conditional on the given label according to updated objective function Eq. 2.

$$\min_G \max_D \mathbb{E}_{x \sim p_{\text{data}}(x)} [\log D(x|c)] + \mathbb{E}_{z \sim p_z(z)} [\log (1 - D(G(z|c)))], \quad (2)$$

where we add class label c as the conditional term compared to Eq. 1. Generating synthetic medical data using conditional GAN is gain more practical values in healthcare scenarios, because medical data is usually labeled and this label makes it meaningful for diagnostic purposes, e.g., for classifying if certain patient has the disease (Frangi et al., 2018), and for data augmentation (Chen et al., 2022).

2.2. Federated Learning

Training DL models usually requires a large amount of training data. However, collecting data is challenging in the field of healthcare because healthcare providers, governments, and related medical organizations must pay particular attention to the patient's privacy and guarantee the proper use of their collected data (Price and Cohen, 2019). In this case, limited data in local healthcare institutions is usually biased and unilateral (Wang et al., 2020b), which in turn impede the AI-assisted diagnostic technology in healthcare (Van Panhuis et al., 2014).

FL has been proposed as a promising strategy to facilitate collaboration among several institutions (e.g., medical centers distributed from different geographical locations) to train a global DL model (Konečný et al., 2016). Given the important role of FL plays in leveraging medical data from distributed locations and the practical usage of DL-based synthetic models in medicine, combining them together will help facilitate advancement in medicine. Previous studies try to establish the FedGAN (Rasouli et al., 2020) and explored its robustness in terms of the differential privacy (Augenstein et al., 2019).

In addition, Byzantine-Robust FL is a key challenge in FL deployment, as the clients are barely controllable and typically viewed as an open system. Literature has shown that FL is vulnerable to multiple kinds of adversaries (Bouacida and Mohapatra, 2021; Liu et al., 2022). Example vulnerabilities includes model poisoning attacks (Bhagoji et al., 2019), gradient inversion attacks (Huang et al., 2021), inference attacks (Ying et al., 2020), backdoor attacks (Li et al., 2022), etc.

2.3. Backdoor Attack

In this section, we begin by introducing the general concept of a backdoor attack. Next, we delve into the specific details of backdoor attacks in FL and backdoor attacks in generative models.

General concept. The backdoor attackers aim to embed a backdoor, also known as trigger, in the training data in order to corrupt the performance of the Deep Neural Network. Given it involves poisoning data, it belongs to the fields of data poisoning attacks, which has been widely explored in multiple machine learning fields, including Support Vector Machines, Statistical Machine Learning, and DL (Biggio et al., 2012; Nelson et al., 2008). In DL, current studies mainly explore poisoning attacks in centralized classification models, where a hidden trigger is pasted on some of the training data with wrong labels. The attacker activates it during the testing time so that the classification model produces a lower testing accuracy for images with triggers (Saha et al., 2020). This attack strategy takes advantage of the tendency that the deep neural network is more likely to

learn the pattern of the backdoor instead of the actual image (Li et al., 2022).

Backdoor attack in FL. Due to the distributed nature of FL, the server has little control on the client side. Namely, FL is even more vulnerable to backdoor and poisoning attacks. Existing studies have explored such attacks in classification models from various perspectives. Bagdasaryan et al. (2020) proposed to use apply *model replacement* as a means to introduce backdoored functionality into the global model within FL. Fang et al. (2020) introduced the initial concept of local model poisoning attacks targeting the Byzantine robustness of FL. Wang et al. (2020a) introduced a novel concept of an *edge-case backdoor*, which manipulates a model to misclassify seemingly straightforward inputs that are highly unlikely to be part of the training or test data. Sun et al. (2019) conducts a thorough investigation of backdoor attacks and defense strategies in FL classification models

Backdoor attack on GAN. The existing backdoor attack has been focusing on classification models. Despite this, the applicability of backdoor attacks against GANs is underexplored, especially in the field of medicine. This is due to the fact that backdoor attacks against GANs are more complex, since the input for GANs is a noise vector, while the output is a generated-new-image. Backdoor in FL for classification models was initially introduced by Bagdasaryan et al. (2020), where a constrain-and-scale technique is applied to amplify the malicious gradient of clients. In the study, the local clients are flexible to employ local training procedures. However, this scenario is unlikely to happen in the medical circumstances, given the organizer of the FL can enforce the proper training procedure on reliable hardware to prevent malicious clients from taking adversarial actions (Pillutla et al., 2019). In contrast to the previous backdoor federated classification study, we assume that there is a reliable FL pipeline that each client follows the provided training rules to calculate and update the correct parameters without modifying them, thereby performing the given training process in accordance with the instructions given by the trusted server (the organizer of the FL in reality). Then we investigate how backdoor attack can affect GAN for data synthesis in this FL setting.

2.4. Defending Backdoor Attack

There are a variety of defense strategies for backdoor attacks ranging from data level to model level but with a focus on the classification models in centralized training. Data level defenses mainly include two perspectives: 1) Detect the trigger pattern and either eliminate it from the data or add a trigger blocker to decrease the contribution of the backdoor during training the DL model (Doan et al., 2020). 2) Perform a series of data argumentation (e.g., shrinking, flipping) before feeding the data into the model (Qiu et al., 2021; Villarreal-Vasquez and Bhargava, 2020). This is because the transitional backdoor attack is sensitive to the pattern of the trigger and the location of the backdoor patch (Li et al., 2021b).

There are more model-level defense strategies: 1) Reconstructing attacked model strategy. This strategy aims to retrain

the trained attacker model with some benign samples to alleviate the backdoor attacks. 2) Synthesis trigger defencing strategy. It attempts to perform outlier detection on the DL models by reconstructing either the specific trigger (Wang et al., 2019; Harikumar et al., 2020) or the trigger distribution (Zhu et al., 2020; Guo et al., 2020). 3) Diagnosing attacked model through meta-classifier. This method applies certain pre-trained classifiers to identify the potentially infected models and prevent deploying them (Kolouri et al., 2020; Zheng et al., 2021). 4) Unlearning the infected model. The unlearning strategy first detects the malicious behavior and then defends against the backdoor attack by performing reverse learning through utilizing the implicit hypergradient (Zeng et al., 2021a) or modifying the loss function (Li et al., 2021a). 5) Robust aggregation. This strategy is specifically tailored for FL. It involves meticulous adjustments of the server aggregation learning rate, taking into account client updates on a per-dimension and per-round basis (Pillutla et al., 2019). 6) Adversarial distillation. This defense strategy is also designed for classification tasks in FL. It employs a GAN on the server side to acquire a distillation dataset. Subsequently, knowledge distillation is applied, utilizing a clean model as the teacher to educate the server model and remove the backdoored neurons from the malicious model (Zhu et al., 2023). 7) Trigger inverse engineering. This is a provable technique that is proposed specifically for backdoor attacks under FL classification models (Zhang et al., 2022).

It requires the benign clients to apply trigger inversion techniques in the training time to construct an augmented dataset that consists of poisoned images with clean labels. This serves as model hardening and reduces the prediction confidence of backdoored sample. The inference step then takes advantage of this prediction confidence to perform classification tasks.

Moreover, the comprehensive backdoor attack surveys can be found in Li et al. (2022) and Guo et al. (2022).

Unfortunately, most of the above defense strategies do not fit the FedGAN settings, either due to the server cannot access the local private data, or the training of GAN-based generative models does not behave the same as the classification models.

3. Methods

The goal of medical image synthesis is to generate high-quality synthetic data that can be employed for open research to argue the limited datasets and balance the training data, and finally hasten DL methodological advancements in medicine. In our study, we explore conditional GAN in the FL setting, i.e., conditional FedGAN.

In this section, we first introduce our setting for FedGAN in Section 3.1 Next, we discuss the scope for adversarial attacks and determine the best way to implement the backdoor attack that involves data poisoning in Section 3.2. Then, we suggest the potential strategies for defending against such attack in FedGAN to build a robust FL system in Section 3.3.

3.1. Federated Generative Adversarial Network

Motivated by the local model poisoning attacks in Byzantine-robust FL classification models proposed in Fang et al. (2020),

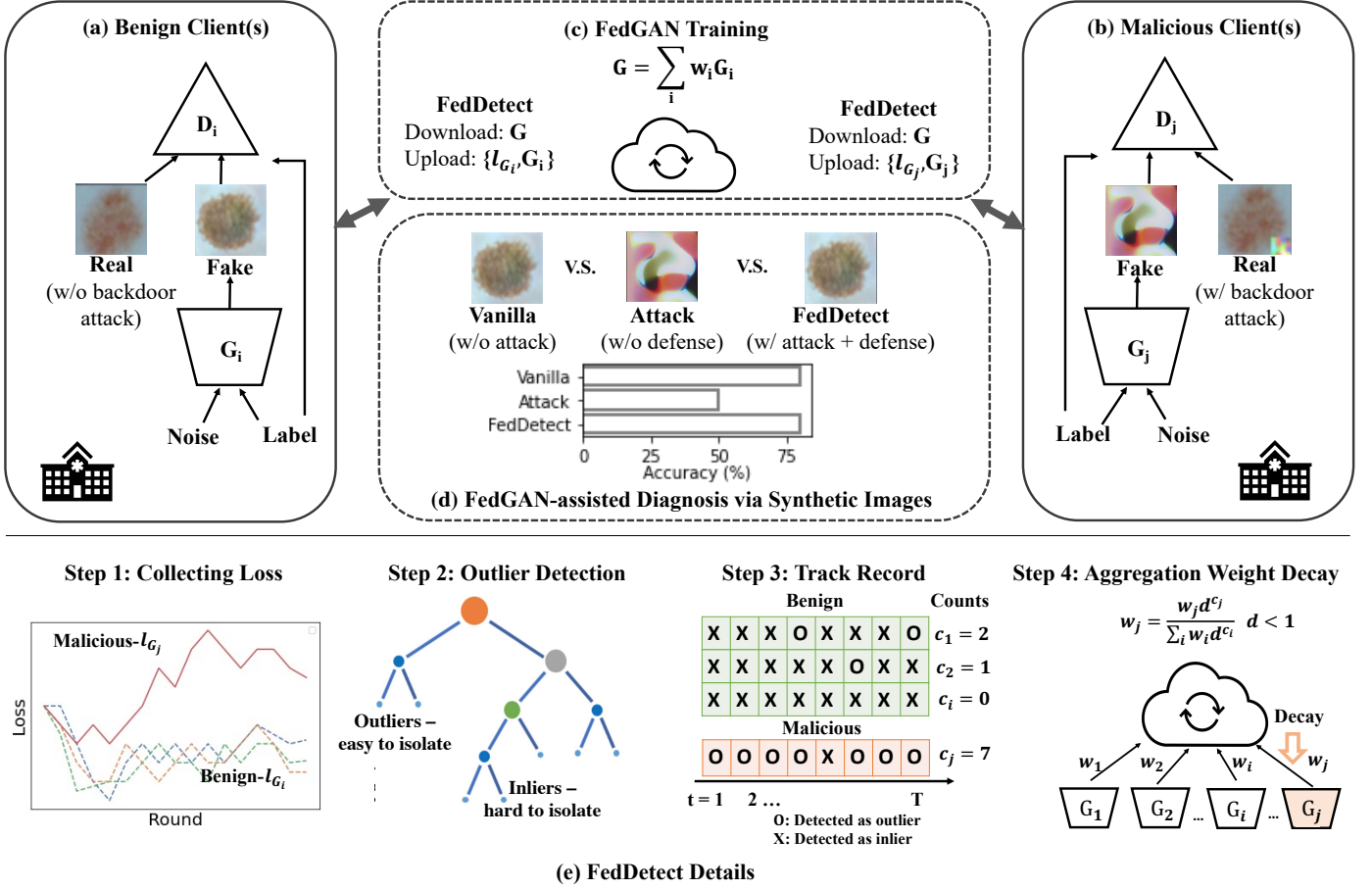


Fig. 2: The overview of our proposed framework. Specifically, our FedGAN scenario consists of benign clients shown in (a), malicious clients shown in (b), and a global conditional FedGAN server as illustrated in (c). During the training, the malicious discriminator is fed with poisoned images. The discriminator and generator are trained against each other locally following the training protocol enforced by the FedGAN organizer. The generators upload their training loss and aggregate parameters per global iteration as described in (c). In the end, we expect the server generator to produce high-quality images for medical research in terms of fidelity and diversity to assist medical diagnosis tasks as demonstrated as Vanilla in (d). However, the attack degrades the central generator’s performance, generating noisy images with little value for medical diagnosis. We propose FedDetect to defend against such attack. As illustrated in (e), FedDetect consists of four steps. First, the FL server collects the local generator loss and then passes them to the isolation forest for anomaly detection. Because outliers are located distantly from inliers, they are supposed to be isolated at the early stage in the construction of the isolation trees. The outliers are flagged as potential adversarial and the server tracks the record of the number of each client being flagged. Finally, the FedGAN server decays the weight of those potential malicious clients based on the track record per round.

we depict the framework of FedGAN using a commonly FL training strategy that averages the shared model parameters, FedAvg (McMahan et al., 2017), in Fig. 2. As introduced in Section 2.2 that studies have extensively explored gradient inversion attacks and inference attacks to infer or reconstruct the inputs of FL models given the shared model parameters, exposing FL training in privacy risk. In light of this, we keep the discriminators (binary classification neural networks) in GAN updating locally as they have direct access to clients’ private data, making them vulnerable to data leakages if their gradients are inverted or inference attacks are used in FL training (Huang et al., 2021). Our FedGAN framework only exchanges generator’s parameters with the server and uses FedAvg to update the global generator. To this end, our FedGAN locally trains both discriminator and generator pairs and globally shares generators’ parameters, which is motivated from Chang et al. (2020).

Formally, we assume that a trusted central generator G_{server} synthesizes images from a set of N federated clients. Each

client C_i , for $i \in [N]$ consists a locally trained discriminator D_i , and a generator G_i . G_i takes random Gaussian noise z and conditional label \tilde{y} as inputs to generate synthetic images, and D_i distinguish the synthetic image $\tilde{x} = G(z, \tilde{y})$ v.s. private image x and its real label y . We keep D_i locally and adopt FedAvg McMahan et al. (2017) to aggregate G_i to G_{server} , namely,

$$G_{\text{server}} = \sum_{i=1}^N w_i G_i, \quad (3)$$

where w_i is a coefficient for weighted averaging. At the end, our federated GAN generate synthetic medical data $G_{\text{server}}(z, \tilde{y}) \sim p_{\text{data}}$ on the server side.

As a valid assumption in the FL system among medical centers, we assume every client, including those malicious ones, follows the given training protocol. For instance, they compute gradients correctly as instructed by the server and update the exact parameters when needed. By requiring FL computa-

Algorithm 1 FedDetect

Notations: Clients C indexed by i ; local discriminator D_i , and generator G_i , local generator loss l_{G_i} , global generator G_{server} , aggregation weight $w_i \in [0, 1]$; times of being detected as malicious i -th client c_i , local updating iteration K ; global communication round T , total number of clients N , decay rate d , warmup iteration m .

```

1:  $c_i \leftarrow 0, w_i \leftarrow \frac{1}{N}$  ▷ Initialization
2: For  $t = 0 \rightarrow T$ , we iteratively run Procedure A then Procedure B
3: procedure A. CLIENTUPDATE( $t, i$ )
4:    $G_i(t, 0) \leftarrow G_{\text{server}}(t)$  ▷ Receive global generator weights update
5:   for  $k = 0 \rightarrow K - 1$  do
6:      $D_i(t, k + 1) \leftarrow \text{Optimize } \ell_D(D_i(t, k), G_i(t, k))$  ▷ Update  $D$  using Eq. (4)
7:      $G_i(t, k + 1) \leftarrow \text{Optimize } \ell_G(D_i(t, k + 1), G_i(t, k))$  ▷ Update  $G$  using Eq. (5)
8:   end for
9:   Send  $G_i(t, K)$  and  $l_{G_i}$  to SERVEREXECUTION
10: end procedure
11: procedure B. SERVEREXECUTION( $t$ ):
12:   for each client  $C_i$  in parallel do
13:      $G_i, l_{G_i} \leftarrow \text{CLIENTUPDATE}(t, i)$  ▷ Receive local model weights and loss.
14:     if  $t > m$  then ▷ Start detection after warmup
15:        $O \leftarrow \text{ISOLATIONFOREST}(\ell_{G_1} \dots \ell_{G_N})$ 
16:       if  $0 < |O| < \frac{1}{2}|N|$  then ▷ Detect valid number of outliers
17:         for each detected client  $C_i$  in  $O$  do
18:            $c_i \leftarrow c_i + 1$  ▷ Increment total count  $C_i$  been detected as outlier
19:            $w_i \leftarrow w_i \times d^{c_i}$  ▷ Decay weights for outliers
20:         end for
21:       end if
22:     end if
23:   end for
24:    $w_i \leftarrow \frac{w_i}{\sum_{i \in [N]} w_i}$  ▷ Normalize weights
25:    $G_{\text{server}}(t + 1) \leftarrow \sum_{k \in [N]} w_k G_i(t)$  ▷ Aggregation on server
26: end procedure

```

tions to be carried out on trusted hardware, this can be accomplished (Pillutla et al., 2019).

3.2. Backdoor Attack Strategies

Backdoor attack is a training time attack that embeds a backdoor into a model by poisoning training data (e.g., adding triggers on the images). The state-of-the-art backdoor attacks focus on image classification model (Chen et al., 2017; Liu et al., 2020) and has been recently studied on FL (Bagdasaryan et al., 2020). Current studies of backdoor attacks in deep generative models (e.g., GAN) train on a poisoned dataset (Rawat et al., 2021) or input a poisoned noise vector (Salem et al., 2020) into the generator so that GAN failed to produce quality synthetic images with similar distribution as the real data. As injecting backdoor to images has been shown more effective (Rawat et al., 2021), we suggest a way of attacking federated GAN only through the poisoned data with more details below.

Adversarial Goals. The objective of the attacker performing a backdoor attack is to corrupt the Byzantine-robust FedGAN (Cao et al., 2020), leading to model divergence or converging to sub-optimal. In FL settings, adversarial clients attack the server generator using poisoned images as the input of discriminator so that the generator can be fooled, no longer generating fake medical-valued images \tilde{x} with high fidelity. That is, $p_{(\tilde{x}|y)} \neq p_{(x|y)}$, for x as real image and y as the corresponding real label.

Adversarial Capabilities. As mentioned in Section 3.1 that a robust FL pipeline includes a trusted server (the organizer of the FL), which has control over the local training process. Thus, the only room for attack is through providing poisoned data to the local discriminator as shown in Fig. 2.

Adversarial Motivation. A vanilla GAN optimizes loss function in the manner outlined in Goodfellow et al. (2014), where the discriminator seeks to maximize the accuracy of the real and fake image classification while the generator seeks to minimize the likelihood that its generated image will be classified as fake. We assume the data of all the clients are from the same distribution, i.e., $x \sim p_{\text{data}}(x)$. We sample noise vectors z from multivariate Gaussian distribution $p_z(z)$. Specifically, the objective is written as follows. In each iteration, for each local discriminator D_i with $i \in [N]$ as the index of i -th client, we perform the local optimization for updating discriminators model parameters when global generator G 's parameters are fixed:

$$\max_{D_i} \mathbb{E}_{x \sim p_{\text{data}}(x)} [\log D_i(x|y_i)] + \mathbb{E}_{z \sim p_z(z)} [\log (1 - D_i(G(z|y_i)))]. \quad (4)$$

Then, we optimize the generator G_i with D_i fixed by

$$\sum_{i=1}^N w_i \min_{G_i} \mathbb{E}_{z \sim p_z(z)} [\log (1 - D_i(G_i(z|y_i)))], \quad (5)$$

then aggregate the global generator G using FedAvg (McMahan et al., 2017) as shown in Eq. (3).

The optimization of GAN is recognized to be difficult, nevertheless, because the generator is subpar upon learning that $\log(D(G(z|y)))$ is probably overfitting given the fact that the discriminator is easy to fit (Goodfellow et al., 2014). Based on the observation and motivated by the backdoor attacks that fool the classifier to memorize (i.e., overfit) the triggers in the classification settings, we implement the trigger following the overfitting principle into the discriminator of FedGAN’s training. The following part gives a detailed explanation of our adversarial model.

Adversarial Model. Following the realistic setting discussed in Bhagoji et al. (2019), we assume that the malicious clients are the minority of the FL participants since the purpose of FL is to augment the training data and it is meaningless to lose trust among the majority of clients. Formally, our threat model contains a set of M adversarial clients, where $|M| = \alpha|N|$ and $0 < \alpha < 0.5$. For every adversarial client, C'_i , the attacker is able to add a trigger δ to every sample in its training set $x \in \mathcal{D}_i$. The goal of the attacker is to fool the central server generator to produce corrupted images that do not have medical research value.

3.3. Defense Strategy

As introduced in Section 2.4, the existing defense strategies focus on classification models, ranging from model level to data level. As data are not accessible in FL, model level defense is desired, where a model level detector is built to find the adversarial behavior and refrain it from training with others (Guo et al., 2021), known as *malicious detection*. Apart from detection, *robust training* is another approach that refines training protocol Ozdayi et al. (2021). To the best of our knowledge, *no existing study* addresses the defense for FedGAN. In this section, we introduce an efficient and effective defense method, FedDetect.

3.3.1. Defender’s capabilities

Let’s recall from our setting that a trusted server and more than half of the benign clients are part of our trusted FL pipeline. The benign server has access to the *model parameters* and requests *training loss*. Note that sharing training loss barely impacts data privacy. At the same time, the server cannot access the local data in any form given the privacy enforcement. Furthermore, the FedGAN server has control over the aggregation process, e.g., performs anomaly detection through locally updated information and assigns suspicious clients low weights to finally exclude them.

Our defense strategy is motivated by the observation that models with backdoor attacks tend to overfit the trigger rather than the actual image (Bagdasaryan et al., 2020). Specifically, in GAN’s training, the discriminator overfits the trigger and perfectly classifies fake and real images, while the generator does not receive effective feedback from the discriminator and then yields high loss and even diverges. Mathematically, as the discriminator overfits on the trigger, $\log(1 - D(G(z|y)))$ in equation 5 will ultimately over-shots and corrupt the performance

of GAN. The locally corrupted GAN gradually contaminates other benign clients through the global aggregation. To this end, we propose to defend against backdoor attacks from the global level by leveraging malicious detection.

3.3.2. FedDetect

Our proposed defense strategy is based on two key observations:

- The malicious clients with poisoning images can easily overfit discriminating the triggers, resulting in worse generator training performance.
- In backdoor attacks, the benign clients’ model updates and loss patterns from a client in multiple iterations are consistent.

Suspicious clients detection Based on the above two observations, the assumption that malicious clients are the minorities of the system and the FL setting (i.e., generators G_i are shared and discriminator D_i ’s information is kept locally) discussed earlier, we suggest performing anomaly detection using the generator loss for client C_i at iteration t specified as

$$\ell_{G_i}^{(t)} = \mathbb{E}_{z \sim p_z(z)} [\log(1 - D_i^{(t)}(G_i^{(t)}(z|y_i)))]. \quad (6)$$

Then, Isolation Forests Liu et al. (2008) is used for anomalous clients detection in every epoch on the generator losses $\mathcal{L} = \{\ell_{G_1}, \dots, \ell_{G_N}\}$. \mathcal{L} is then sent to the isolation forest for anomaly detection, which consists of two stages: fitting and predicting. The fitting stage is described in Algorithm 2. It constructs isolation trees (iTrees) through recursively partitioning \mathcal{L} (line 6-7) until reaching a sub-sampling size ϕ (line 3). This way, the potential outliers (points far away from inliers) are expected to be isolated with fewer partitions, which locates in the shallow leaves of iTrees as shown in Fig 2 (e). After constructing isolation forest that consists of a certain number of iTrees, it reaches the predicting stage, which first computes the single path length $h(\ell_{G_i}) = e + C(n)$ for every uploaded ℓ_{G_i} , where e stands for the number of edges from the root to ℓ_{G_i} in the iTrees and $C(n) = 2H(n-1) - \frac{2(n-1)}{n}$. Ultimately, isolation forest computes the expectation score $Score(\ell_{G_i}) = 2^{-\frac{E(h(\ell_{G_i}))}{C(\phi)}}$. If ℓ_{G_i} has lesser length in most iTrees in the forest, $Score(\ell_{G_i})$ approaches 1, indicating higher possibility that ℓ_{G_i} is an outlier.

To achieve a robust FL system without sacrificing privacy, the server in FedGAN only asks clients to report their loss along with the model parameters of the generator and perform outlier detection on the server-side. Again, in the FL setting for the medical applications, we assume all the clients’ training protocol and reported value is regularized by the launched trustworthy software (Pillutla et al., 2019), thus the shared information is trusted.

Adaptive weights for robust aggregation As the initialization of FL training, we assign every client with an initial weight $w_i = \frac{1}{|N|}$. Starting from epoch m as a warmup, we activate the Isolation Forest Liu et al. (2008) on clients’ losses of generator ℓ_{G_i} to red flag suspicious clients. Recall that there are less than half of malicious clients in our adversarial model. Thus, the valid detection algorithm should produce a set of potential

Algorithm 2 Establish iTree

Notations: \mathcal{L} represents the set of generator loss. ϕ is the sub-sampling size.

```

1: procedure A. ESTABLISH-iTREE( $\mathcal{L}$ )
2:   if  $|\mathcal{L}| \leq \phi$  then                                     ▶ Construct the tree if reached the sub-sampling size.
3:     return Node( $\mathcal{L}$ )
4:   else
5:      $\mathcal{L}_l, \mathcal{L}_r \leftarrow$  split  $\mathcal{L}$  according to certain attribute   ▶ Randomly split point according to certain attribute
6:     return ESTABLISH-iTREE( $\mathcal{L}_l$ )  $\cup$  ESTABLISH-iTREE( $\mathcal{L}_r$ )           ▶ Recursively partition to form iTree
7:   end if
8: end procedure

```

malicious clients O , where $|O| < \frac{1}{2}|N|$. We perform malicious detection per global iteration and keep track of the number of ‘malicious’ red flags assigned to each client C_i over the training process, denoting as counter c_i . In each global iteration, the adaptive aggregation weight of clients detected as an outlier will decay according to a decay constant $d \in (0, 1)$ and the total time it has been detected c_i by $w_i^{(t+1)} = w_i^{(t) \times d^{c_i}}$. Namely, if a client is more frequently detected as malicious, it receives a smaller aggregation weight. We further normalize the weights. The detailed algorithm is described in Algorithm 1.

4. Experiments

This section presents experiment settings and results of backdoor attacks, FedDetect, state-of-the-art (SOTA) defense practices for FedGAN and FedGAN-assisted diagnoses based on two publicly available medical datasets. Section 4.1 introduces the details of both datasets and our FedGAN pipeline. Section 4.2 explores the effect of backdoor attack on both datasets with different types and sizes of triggers. Section 4.3 implements FedDetect and compare it with SOTA. Finally, section 4.4 trains a diagnostic model with different combinations of real data with vanilla, attack, and defense data to examine our FedGAN’s performance in the medical scenario.

4.1. Experimental Settings

4.1.1. Datasets

We experiment our FedGAN model on one RGB dataset and one black-white single-channel dataset.

ISIC Dataset The International Skin Imaging Collaboration (ISIC) dataset (Codella et al., 2018) is a dataset for skin lesion classification widely used for proof of concept in medical image analysis. Our training set for all the clients of FedGAN contains 1800 Benign samples and 1497 Malignant samples. In our FedGAN, 824 randomly sampled images are assigned to each of the three clients and the last client gets 825 images. All images are resized to 256×256 before being fed into the FedGAN. We present sample ISIC images in Fig. 3 (a).

Chest X-Ray Dataset (Pneumonia) ChestX (Kermany et al., 2018) contains 5856 gray-scale images. In our FedGAN, 1464 images are randomly sampled for each client. All images are also resized to the size of 256×256 as the ISIC dataset. The samples are present in Fig. 4(a).

4.1.2. Generative Adversarial Networks:

Our conditional FedGAN follows the recipe of DC-GAN (Radford et al., 2015), one of the most widely used conditional GAN frameworks, as our basic network. We replace the generator architecture of DCGAN with that of StyleGAN2-ADA (Karras et al., 2020), given its generator produces images with high qualities in the majority of datasets and has great potential to generate high-resolution medical images for clinical research (Woodland et al., 2022). It is worth noting that the attack and defense strategies although demonstrated with our selected architecture, they have the potential to apply to other GAN-based generative models. In all training scenarios, we adopt the Adam optimizer with a learning rate of 2×10^{-4} for both the generator and the discriminator. The batch size is set to 32 as per the limit of a 32GB Tesla V100 GPU.

4.1.3. Federated Learning

Considering the total available sample size and the limitation of our GPU and hardware memory, we run FedGAN on four clients where each client is trained on randomly equally sampled images from the datasets described above. This study serves as a first step towards understanding backdoor attacks and exploring defense strategies in FedGAN training for medical image synthesis. We contend scale of simulation is still significant and can easily be generalized to a larger scale. We update the local generator parameters to the global server every local epoch and train the FedGAN with 200 global epochs using FedAvg McMahan et al. (2017). The synthetic medical images with vanilla FedGAN (no attack and defense induced) are presented in Fig. 3 (b) for ISIC dataset and Fig. 4 (b) for ChestX dataset.

4.2. Backdoor Attack on FedGAN

4.2.1. Backdoor Details

As mentioned in Section. 4.1.3, four clients are simulating four medical institutions in our FedGAN setting and each client is trained on equally sampled data from the original training dataset. Among the four clients, one is randomly selected as the malicious client. The three benign clients are trained with normal images, while the malicious client is trained with poisoned images. As for the poisoned images, different triggers are applied for ISIC and ChestX datasets as detailed below based on their modalities.

Backdoor on ISIC We apply the trigger strategy proposed by Saha et al. (2020), which has shown to be effective for back-

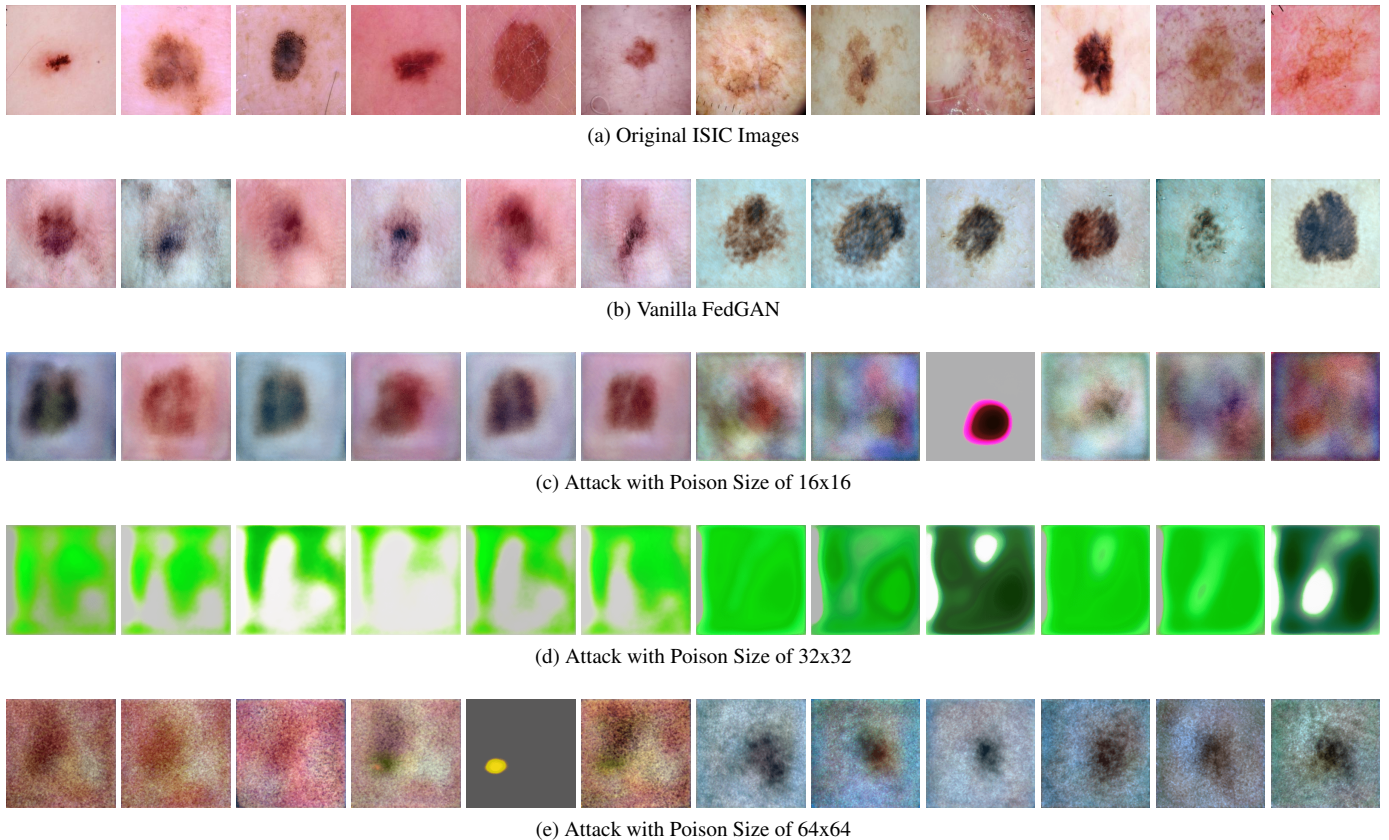


Fig. 3: Visualization on ISIC Attacking

Table 1: Quantitative Comparison for Attack. ↓ indicates the smaller the better.

Settings	ISIC			
	Vanilla GAN	Attack		
		16x16	32x32	64x64
LPIPS (Benign) ↓	0.6735	0.7005	1.0373	0.7187
LPIPS (Malignant) ↓	0.7354	0.9248	1.0337	0.7984

door attacks in classification tasks. Specifically, we adopt a random matrix of colors that has a different pattern from the actual image with sizes ranging from 16×16 (only 0.39% of the size of the original image) to 64×64 . The same trigger is pasted onto the bottom right of all the training images in the malicious client before launching FedGAN training. The examples of poisoned images are shown in Fig. 2, which are fed into the discriminator D of malicious clients.

Backdoor on ChestX ChestX is a gray-scale image dataset and it will be inappropriate to use the same trigger as the ISIC dataset. In this case, we attempted to use a white square as the trigger. All the rest settings are the same as above, including the sizes of the trigger starting from 16 to 64×64 and its location is on the bottom right of the image.

4.2.2. Metrics

In addition to the qualitative evaluation of the fidelity of synthetic images, we have also included the Learned Perceptual Image Patch Similarity (LPIPS) to quantitatively evaluate the

them Zhang et al. (2018). LPIPS assesses the perceptual similarity between two pictures. In essence, LPIPS determines how comparable two picture patches' activations are for a given network. In our experiments, we use AlexNet as the neural network. This measurement has been demonstrated to closely reflect human perception (Wang et al., 2020c). Image patches with a low LPIPS score are perceptually similar. We have also run the classification experiments in Section 4.4 to measure the influence of attack directly on training Deep Neural Networks.

4.2.3. Attack Result and Analysis

Visualization Results The visualization of the original images for both datasets are shown in Fig 3(a) and Fig 4(a). The generated images are shown in Fig. 3(b) and Fig 4(b). In both Fig 3 and Fig 4, (c), (d) and (e) presents the attacked images with poison size of 16x16, 32x32 and 64x64 individually for both datasets. The virtualization plot shows that the appearances of the attacked images are significantly different from those generated images in row (b), which means that essential disease-

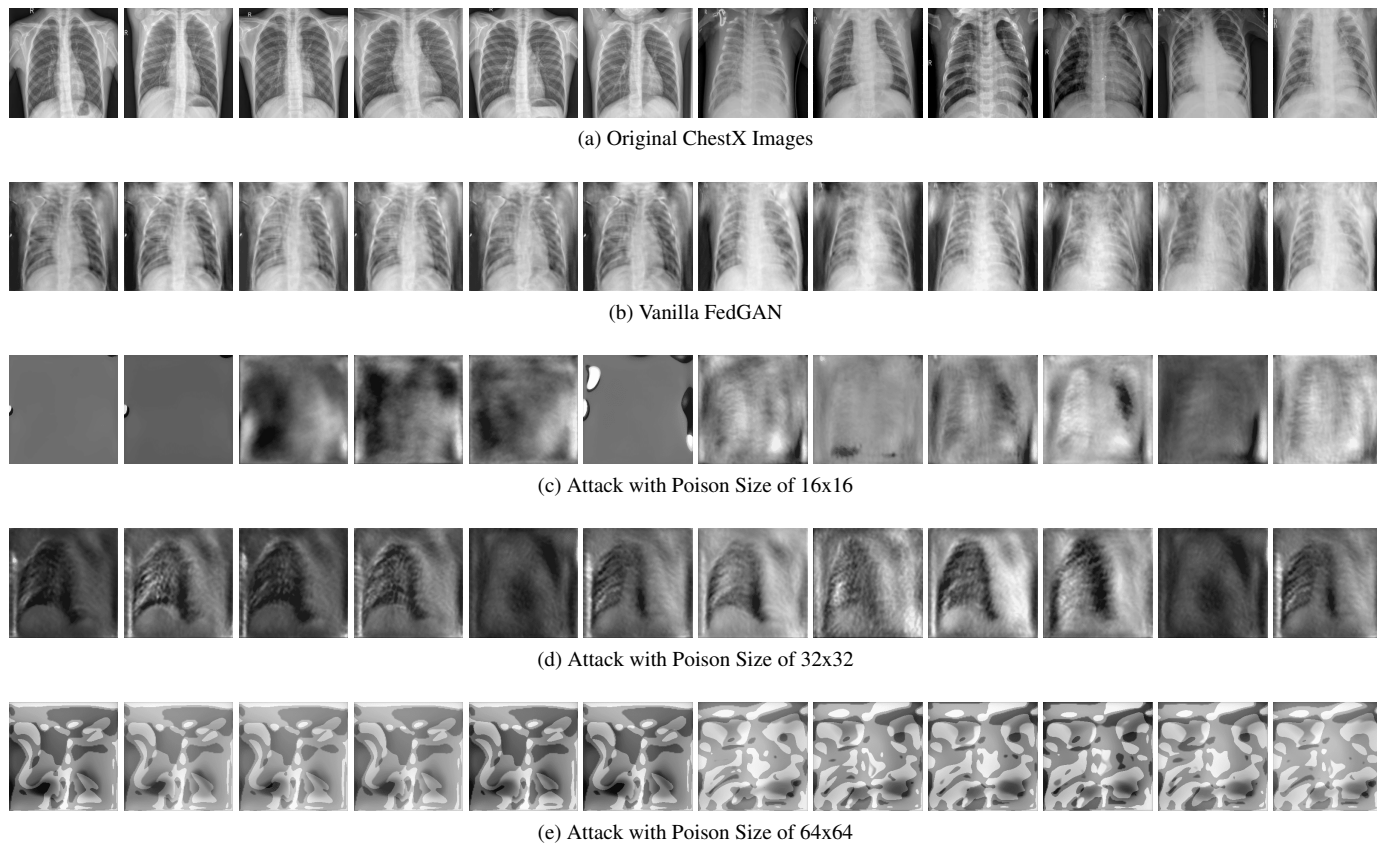


Fig. 4: Visualization on ChestX Attacking

Table 2: Quantitative Comparison for Attack. ↓ indicates the smaller the better.

Settings	ChestX			
	Vanilla GAN	Attack		
		16x16	32x32	64x64
LPIPS (Normal) ↓	0.3748	0.7479	0.6193	0.6042
LPIPS (Pneumonia) ↓	0.4158	0.5968	0.6327	0.6165

related information is lost and the images cannot be used for diagnostic reasons. Furthermore, we find that the strongest assault, which completely ruins FedGAN performance, has a poison size of 32x32 for the ISIC dataset and 64x64 for the ChestX dataset. As the discriminator in our FedGAN is consistently maintained locally, we anticipate that the poisoned data will first directly impact the performance of the discriminator, yielding a sub-optimal discriminator. This subsequently affects the generator through adversarial training, which, in turn, contaminates other FL participants during server aggregation. Consequently, the size of the trigger has a limited direct impact on the strength of the attack, as the poisoned dataset only indirectly affects the entire system. However, we perform the ablation study for trigger sizes to demonstrate the generalizability of our attacks and defenses.

Quantifying Image Fidelity For most attacked images, we are able to observe a significant contrast and distortion from the benign images. In both datasets, we also report LPIPS values. The

smaller the LPIPS, the more similar the two images. The quantitative metrics match what we observed, where the attacked images have higher LPIPS values than those of vanilla images, indicating that there is less similarity between the generated images with the original datasets than the vanilla GAN generated images. As shown in Table 1 and Table 2, the LPIPS significantly increases for both datasets. The 32x32 patch achieves the strongest attack, in which the LPIPS score increases 54% compared to the Vanilla FedGAN. For the ChestX dataset, all LPIPS score for normal samples almost doubles compared to the Vanilla GAN, indicating the large gap in the similarity between the original images and the generated images.

4.3. Defense Result and Analysis

When the malicious clients train on contaminated data in the attack outlined in Section 4.2, the discriminator soon overfits the trigger and causes the entire FedGAN model to suffer from training instability. Here, we try to carry out FedDetect to counter this threat and compare it with several alternatives.

4.3.1. Baseline Defense Strategies

As summarized in Section 2.4, state-of-the-art defense practices are made up of data level and model level. Data level defenses include adding trigger blockers, eliminating backdoors from the training data, and data argumentation. Due to the privacy regulations of FL, FedGAN is unable to record the clients' training data; as a result, the deleting trigger strategy is not applicable. Also, the existing defense strategies focus on classification models.

Among the model level defense strategies, the majority of them also fail under the FedGAN pipeline. For example, *the diagnostic approach* requires a certain pre-trained meta-classifier (Kolouri et al., 2020; Xu et al., 2021), which is inappropriate for GAN's scenario, where the discriminator and the generator need to train against each other at the beginning. *The unlearning approach* takes two steps, first, the infected data need to be detected, and then the model will unlearn such data (Li et al., 2021a; Zeng et al., 2021a). This strategy works well for classification tasks given its reversible objective function, but it again does not fit the scenario of GAN, where both the discriminator and the generator train against each other through the minmax loss function as specified in equation 2, which cannot be easily reversed as the classification loss forms. *The trigger synthesis approach* requires the defender to access data information (Wang et al., 2019; Guo et al., 2020). Additionally, because the FedGAN diverged before the trigger was synthesized in our example, the synthesizing trigger practice does not suit the FedGAN discipline.

In the end, we consider the comparison with the data argumentation technique and the model reconstruction strategy that can be compatible with the scenario of FedGAN. We deep dive into both methods in detail below and perform empirical experiments on both methods:

Data Augmentation To the best of our knowledge, Li et al. (2020) first draw the conclusion that the effect of backdoor attack depends heavily on the position and the appearance of triggers. They proposed the spatial transformation-based defense, which modifies the location of the trigger on images, including horizontal flipping and padding after shrinking on the original image. Qiu et al. (2021); Borgnia et al. (2021); Zeng et al. (2021b) further performed more comprehensive data augmentations and validated the efficacy of them in centralized classification models. In our setting, we apply two kinds of data augmentation. Given the backdoor attack is sensitive to the location of the trigger as indicated by Li et al. (2020), we perform the random horizontal flipping on inputs before being fed into the FedGAN in the first experiment. In the second experiment, random rotation is applied. Each image will be randomly rotated within the range of $(-90, 90)$ and then fed into the FedGAN.

Model Reconstruction Model Reconstruction, also known as fine-tuning, aims to retrain the infected DL model with a small amount of benign data to alleviate the effect of backdoor attack (Liu et al., 2017; Li et al., 2022). This strategy is based on the theory of the catastrophic forgetting property of the deep neural networks (Kirkpatrick et al., 2017). Since in FL, each client owns a specific quantity of benign data, thus model reconstruction matches the FedGAN setting. In order to simulate

the scenarios in the reality, we reconstruct the model with a dataset containing 500 real images per class after receiving the trained generator model from the FedGAN server. In this experiment, we fine-tune the innocuous samples with 200 epochs and examine their performance.

Robust Aggregation In FL, the defense against backdoor attacks has recently incorporated the concept of robust aggregation, as demonstrated by techniques such as adjusting the "learning rate" at the server level during the aggregation process (Ozdayi et al., 2021; Pillutla et al., 2019). This approach assumes that the updated gradients from both malicious and benign clients exhibit element-wise sign differences. Consequently, a *threshold* is introduced at the server side, where the loss is maximized (e.g., a process of unlearning) if the sum of the signs falls below this *threshold*. The server utilizes a *server learning rate* to control the step and direction during the aggregation process in order to maximize the loss. Specifically, the *server learning rate* is multiplied by -1 for those dimensions where the sum of the signs is below the *threshold*.

4.3.2. Implementation Details of FedDetect

FedDetect is applied to the global aggregation step on the server side. To ensure robust detection, recall our outlier detection method described in Algorithm 1 requires a warmup process to allow enough time for the malicious clients to overfit the backdoor and behave differently from those benign ones. In our experiments, we set the warmup epoch $m = 10$. After $m > 10$, generators' losses are required to share with the server to perform malicious detection. For the ISIC dataset, a decay constant $d = 0.9$ is used to penalize weights for the clients detected as an anomaly in every epoch using Isolation Forests (Liu et al., 2008). For ChestX dataset, the decay constant $d = 0.8$ is applied in our experiments. We accumulatively count the times of being detected as malicious for each client $c_i(t)$ upon global iteration t , at which the calibrated client weights are decayed by timing $d^{c_i(t)}$. Note in the global aggregation, we normalize w_i so that clients' aggregation weights are sum to 1.

4.3.3. Defense Results and Analysis

For the ISIC dataset, Fig 5 presents the visualization of the defenses experiments and Table 3 provides the corresponding quantitative assessment. For the ChestX, Fig 6 visualizes the effect of all defense strategies and Table 4 presents the corresponding quantitative results.

Visualization Results As visualized in both row (a) of Fig 5 and Fig 6, FedDetect effectively blocks the spread of backdoor attacks from malicious clients and generates images with qualities that are comparable with the vanilla GAN for both ISIC and ChestX in all poisoning trigger sizes. We also visualize the synthetic images generated with FedGAN with the baseline defense methods described in Section 4.3.1, with the results of ISIC in Fig 5 and the results of ChestX in Fig 6. Specifically, row (b) presents the model reconstruction approach, row (c) presents the data augmentation with horizontal flip and random rotation, and row (d) visualizes generated image robust aggregation with different poison sizes. As can be seen in Fig 5, all the baseline defense strategies fail to block the backdoor at-

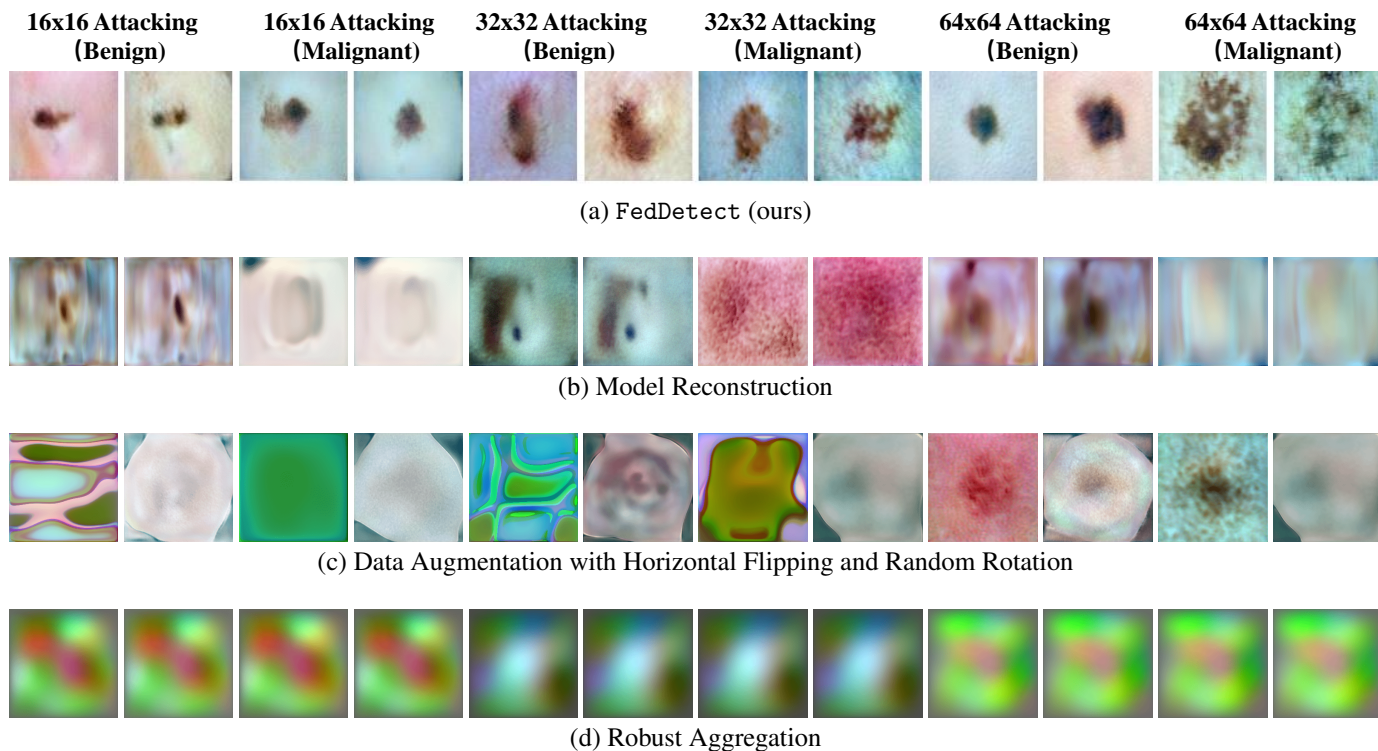


Fig. 5: Visualization on different defense strategies for ISIC

Table 3: Quantitative Metrics of Defense for ISIC. ↓ indicates the smaller the better.

Settings	FedDetect (ours)			Model Reconstruction			Aug: Horizontal Flip			Aug: Random Rotation			Robust Aggregation		
	16x16	32x32	64x64	16x16	32x32	64x64	16x16	32x32	64x64	16x16	32x32	64x64	16x16	32x32	64x64
LPIPS (B) ↓	0.7337	0.6496	0.6754	0.9420	0.8791	0.7961	0.8504	0.9605	0.6883	0.7566	0.8347	0.7468	0.9696	0.9875	1.0412
LPIPS (M) ↓	0.8602	0.7446	0.7502	0.8702	0.5724	0.9553	1.028	0.9454	0.8869	0.8198	0.8846	0.8065	0.9717	0.9910	1.0419

tack in FedGAN for ISIC, where the generated images still mismatch the original image. In ChestX Fig. 6, random horizontal flipping for poison size of 64x64 and random rotation for poison size of 16x16 seems to take effect, which reconstructs the outline of chests. However, this outline is still distorted due to the nature of data argumentation, which may miss important information for diagnostic purposes.

Quantifying Image Fidelity The corresponding LPIPS score is shown in Table 3 for ISIC and Table 4 for ChestX. Our defense strategy results in the lowest LPIPS score for almost all entries, in which FedDetect has an average of 0.73 LPIPS score, smaller than the model reconstruction, augmentation, and robust aggregation, where their LPIPS are 0.84, 0.85 and 1.00 individually for ISIC. Similarly for ChestX, FedDetect reaches a score of 0.41, while model reconstruction has an average of 0.64, data augmentation has 0.65 and robust aggregation has the highest average of 0.7851. These are in accordance with what we observed in the visualization plot that FedDetect generates the most similar image as the vanilla FedGAN. Also, the quantitative data for rows (a) matches the observation that LPIPS score recovers to a similar level as the non-attacked group compared to the attacked group in Fig. 3 and Fig 4.

4.4. Synthetic Image Utility Assessment in Classification Tasks

As described in Method Section 2.2, medical data within one medical institution are usually limited, biased, and private, which creates difficulties in its utility, for example, training regular DL models. We simulate the situation of training a classifier only with data in one intuition. The synthetic medical images generated by FedGAN (and their labels) can serve as data augmentation to improve classifier performance. In this part, we trained two classifiers to show the efficacy of the proposed FedGAN pipeline.

4.4.1. Classifier Architecture and Hyper-Parameter Tuning:

DenseNet121 is applied as the backbone model for training the classifier for both datasets (Huang et al., 2017). All inputs are resized into 224×224 to fit the default model architecture of DenseNet121. We specify the training details for ISIC and ChestX below.

ISIC: The SGD optimizer with a learning rate of 1×10^{-3} and weight decay of 1×10^{-4} is used for classifying the ISIC images. Also, the learning rate is decreased by 0.9 after each epoch. The densenet is trained 20 epochs.

ChestX: The Adam optimizer with a learning rate of 1×10^{-5} is used for training the classifier for the ChestX dataset for 20 epochs. Its learning rate is decayed after each epoch by 0.9.

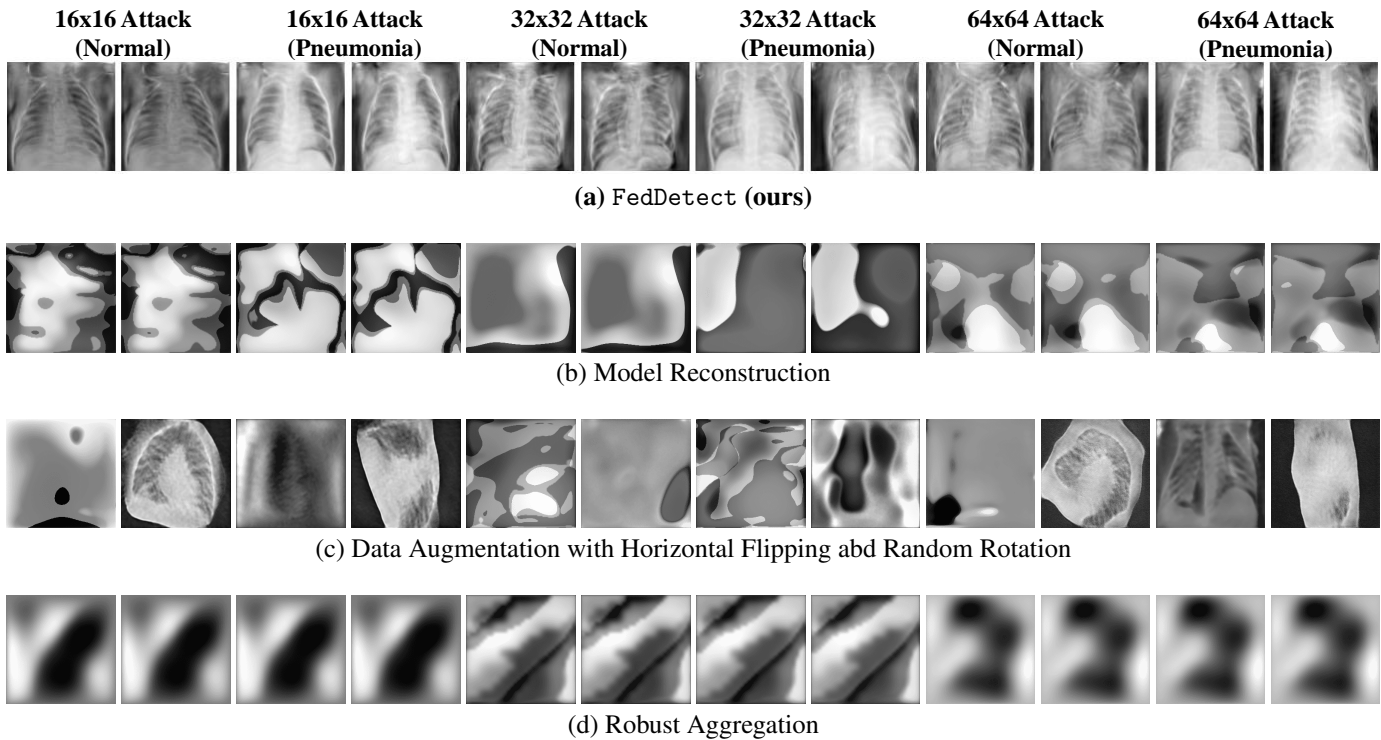


Fig. 6: Visualization on different defense strategies for ChestX

Table 4: Quantitative Metrics of Defense for ChestX. ↓ indicates the smaller the better.

Settings	FedDetect (ours)			Model Reconstruction			Aug: Horizontal Flip			Aug: Random Rotation			Robust Aggregation		
	16x16	32x32	64x64	16x16	32x32	64x64	16x16	32x32	64x64	16x16	32x32	64x64	16x16	32x32	64x64
LPIPS (N) ↓	0.4281	0.3874	0.3892	0.6057	0.7071	0.6154	0.7648	0.6316	0.7767	0.5327	0.6926	0.6311	0.7900	0.7911	0.7897
LPIPS (P) ↓	0.4340	0.4187	0.3940	0.6181	0.6813	0.6240	0.6684	0.6346	0.6231	0.5589	0.7137	0.6212	0.7819	0.7875	0.7706

Also, all input images are augmented by randomly applying horizontal flip and vertical flip.

4.4.2. Data Augmentation with Synthetic Images in Diagnostic Settings

In order to simulate the real-life challenge of training diagnostic DL models, we set up multiple classifiers and fed each with a different number of real samples. The first experiment simulates training a diagnostic classification model only on limited data (e.g., data within one healthcare institution) while the other mimics FedGAN-facilitated training. In both ISIC and ChestX datasets, the first experiment trains the classifier with real images ranging from 1 to 500 per class sampled from our datasets. Then, we augment the real samples above with 1000 FedGAN-generated synthetic images per class.

4.4.3. Metrics

We train the classifiers and evaluate their performance using a pre-processed balanced testing set that contains equal number of samples for each class. In the ISIC dataset, there are 300 Benign samples and 300 Malignant samples. The testing set of ChestX includes 234 Normal images and 234 Pneumonia images. In order to gain robust results, each setting has been executed independently five times with different random seeds.

We report the average test accuracy as well as their standard deviation (std).

4.4.4. Results and Analysis

Fig 7a and Fig 7b present the test accuracy for both datasets. The blue curve, which is labeled as “Real only”, represents the average test accuracy with only real data. The green line, marked as “Unattacked with real”, represents the average test accuracy of FedGAN-assisted training. The “Attacked with real” curve represents the FedGAN with backdoor attack with a patch size of 32x32. The red solid curve represents the backdoor attacked FedGAN with FedDetect defense strategy. The corresponding shadows stand for the std of the test accuracy over five different trials. The x-axis represents the number of real images added to the training set in one classification trial. For training with all real images, the size of the dataset equals the number on the x-axis. For all other training, the size of the training set equals the number of real images on the x-axis plus the number of generated images from FedGAN, which is 1000 images per class for both datasets.

Utility of High Quality Synthetic Data As shown in both figures, the augmented dataset using vanilla FedGAN without attack and backdoor attacked FedGAN with FedDetect gains higher test accuracy than purely the real dataset. This is par-

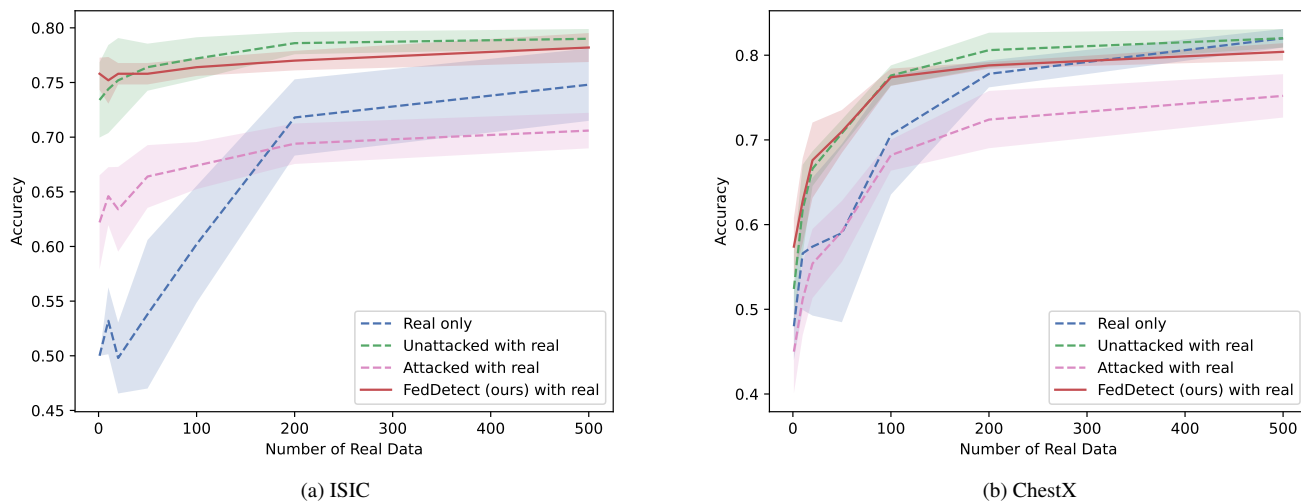


Fig. 7: Classification accuracy on synthetic data augmentation with different number of real training data per class.

ticularly evident for the ISIC dataset, where average test accuracy with the extremely limited training sample (i.e. one sample per class) can achieve 0.73 compared to the random guess results of 0.50 from using the real data only. When we have 500 real data per class, adding the synthetic data generated with FedDetect gains an accuracy of 0.80 compared to the accuracy of 0.73 while using real data only. As for the ChestX dataset, the similar pattern preserves when the real dataset is small (e.g., < 200 samples per class). In addition, for both datasets, the average test accuracy using the synthetic data generated with FedDetect under backdoor attack recovers approximately the same as the vanilla FedGAN without attack, which is represented as the green curve in both graphs. The result indicates that synthetic data with high utility can aid diagnostic retains good performance, given it learns the distribution pattern over multiple decentralized datasets, which finally generates a diverse training dataset. This diversity not only benefits training the deep learning classification, but also provides healthcare practitioners more resources to employ in various ways in reality.

Backdoor Attack Affect Data Utility The effect of augmenting the synthetic data from FedGAN with backdoor attacks is revealed by the orange curves. Seeing from the trend, it lies below all curves for the ChestX dataset, indicating its worst performance. For the ISIC dataset, the attacked images also reach the lowest test accuracy when the real images are greater than 200, which indicates augmenting with low-quality synthetic data from the poisoned generative model even can hurt classification performance.

The classification results corresponds to visualization in the previous Sections 4.2 and 4.3. The attack corrupts the overall performance of FedGAN and FedDetect effectively suppresses the adversarial behavior.

5. Conclusion

Motivated by the idea of backdoor attacks in classification models, this work investigates the pitfalls of backdoor attacks in training conditional FedGAN models. We conduct extensive experiments to investigate the backdoor attack on two public datasets and evaluate among different types and sizes of triggers. Based on our key observations on malicious clients' loss patterns, we propose FedDetect as an effective defense strategy against backdoor attacks in FedGAN. We comprehensively conduct quantitative and qualitative assessments on the fidelity and utility of the synthetic images under different training conditions. We demonstrate the FedDetect significantly outperforms the alternative baselines and preserve comparable data utility as attack-free vanilla FedGAN.

As the first step towards understanding backdoor attacks in FedGAN for medical image synthesis, our work brings insight into building a robust and trustworthy model to advance medical research with synthetic data. Furthermore, we hope to highlight that FedDetect involves only lightweight improvement on the server aggregation step. This makes FedDetect flexible to integrate into different GAN-based federated generative models. Our future work includes scaling up the FL system with more clients, generalizing FedDetect to other deep generative models, e.g., Diffusion models (Song et al., 2021), and considering other variants of backdoor attacks, e.g., frequency-injection based attack Feng et al. (2022).

Acknowledgments

This work is supported in part by the Natural Sciences and Engineering Research Council of Canada (NSERC), Public Safety Canada (NS-5001-22170), and NVIDIA Hardware Award. We thank Chun-Yin Huang and Nan Wang for their kind instruction to Ruinan Jin and assistance with implementation.

References

- Augenstein, S., McMahan, H.B., Ramage, D., Ramaswamy, S., Kairouz, P., Chen, M., Mathews, R., et al., 2019. Generative models for effective ml on private, decentralized datasets. arXiv preprint arXiv:1911.06679 .
- Bagdasaryan, E., Veit, A., Hua, Y., Estrin, D., Shmatikov, V., 2020. How to backdoor federated learning, in: International Conference on Artificial Intelligence and Statistics, PMLR. pp. 2938–2948.
- Bhagoji, A.N., Chakraborty, S., Mittal, P., Calo, S., 2019. Analyzing federated learning through an adversarial lens, in: International Conference on Machine Learning, PMLR. pp. 634–643.
- Biggio, B., Nelson, B., Laskov, P., 2012. Poisoning attacks against support vector machines. arXiv preprint arXiv:1206.6389 .
- Borgnia, E., Cherepanova, V., Fowl, L., Ghiasi, A., Geiping, J., Goldblum, M., Goldstein, T., Gupta, A., 2021. Strong data augmentation sanitizes poisoning and backdoor attacks without an accuracy tradeoff, in: ICASSP 2021-2021 IEEE International Conference on Acoustics, Speech and Signal Processing (ICASSP), IEEE. pp. 3855–3859.
- Bouacida, N., Mohapatra, P., 2021. Vulnerabilities in federated learning. IEEE Access 9, 63229–63249.
- Buczak, A.L., Babin, S., Moniz, L., 2010. Data-driven approach for creating synthetic electronic medical records. BMC medical informatics and decision making 10, 1–28.
- Cao, X., Fang, M., Liu, J., Gong, N.Z., 2020. Fltrust: Byzantine-robust federated learning via trust bootstrapping. arXiv preprint arXiv:2012.13995 .
- Chang, Q., Qu, H., Zhang, Y., Sabuncu, M., Chen, C., Zhang, T., Metaxas, D.N., 2020. Synthetic learning: Learn from distributed asynchronous discriminator gan without sharing medical image data, in: Proceedings of the IEEE/CVF Conference on Computer Vision and Pattern Recognition, pp. 13856–13866.
- Chen, R.J., et al., 2021. Synthetic data in machine learning for medicine and healthcare. Nature Biomedical Engineering 5, 493–497.
- Chen, X., Liu, C., Li, B., Lu, K., Song, D., 2017. Targeted backdoor attacks on deep learning systems using data poisoning. arXiv preprint arXiv:1712.05526 .
- Chen, Y., Yang, X.H., Wei, Z., Heidari, A.A., Zheng, N., Li, Z., Chen, H., Hu, H., Zhou, Q., Guan, Q., 2022. Generative adversarial networks in medical image augmentation: a review. Computers in Biology and Medicine , 105382.
- Codella, N.C., Gutman, D., Celebi, M.E., Helba, B., Marchetti, M.A., Dusza, S.W., Kallou, A., Liopyris, K., Mishra, N., Kittler, H., et al., 2018. Skin lesion analysis toward melanoma detection: A challenge at the 2017 international symposium on biomedical imaging (isbi), hosted by the international skin imaging collaboration (isic), in: 2018 IEEE 15th international symposium on biomedical imaging (ISBI 2018), IEEE. pp. 168–172.
- Doan, B.G., Abbasnejad, E., Ranasinghe, D.C., 2020. Februus: Input purification defense against trojan attacks on deep neural network systems, in: Annual Computer Security Applications Conference, pp. 897–912.
- Dube, K., Gallagher, T., 2013. Approach and method for generating realistic synthetic electronic healthcare records for secondary use, in: International Symposium on Foundations of Health Informatics Engineering and Systems, Springer. pp. 69–86.
- Fang, M., Cao, X., Jia, J., Gong, N., 2020. Local model poisoning attacks to {Byzantine-Robust} federated learning, in: 29th USENIX Security Symposium (USENIX Security 20), pp. 1605–1622.
- Feng, Y., Ma, B., Zhang, J., Zhao, S., Xia, Y., Tao, D., 2022. Fiba: Frequency-injection based backdoor attack in medical image analysis, in: Proceedings of the IEEE/CVF Conference on Computer Vision and Pattern Recognition, pp. 20876–20885.
- Frangi, A.F., Tsafaris, S.A., Prince, J.L., 2018. Simulation and synthesis in medical imaging. IEEE transactions on medical imaging 37, 673–679.
- Goodfellow, I., Pouget-Abadie, J., Mirza, M., Xu, B., Warde-Farley, D., Ozair, S., Courville, A., Bengio, Y., 2014. Generative adversarial nets. Advances in neural information processing systems 27.
- Guo, W., Tondi, B., Barni, M., 2021. An overview of backdoor attacks against deep neural networks and possible defences. arXiv preprint arXiv:2111.08429 .
- Guo, W., Tondi, B., Barni, M., 2022. An overview of backdoor attacks against deep neural networks and possible defences. IEEE Open Journal of Signal Processing .
- Guo, W., Wang, L., Xu, Y., Xing, X., Du, M., Song, D., 2020. Towards inspecting and eliminating trojan backdoors in deep neural networks, in: 2020 IEEE International Conference on Data Mining (ICDM), IEEE. pp. 162–171.
- Harikumar, H., Le, V., Rana, S., Bhattacharya, S., Gupta, S., Venkatesh, S., 2020. Scalable backdoor detection in neural networks, in: Joint European Conference on Machine Learning and Knowledge Discovery in Databases, Springer. pp. 289–304.
- Huang, G., Liu, Z., Van Der Maaten, L., Weinberger, K.Q., 2017. Densely connected convolutional networks, in: Proceedings of the IEEE conference on computer vision and pattern recognition, pp. 4700–4708.
- Huang, Y., Gupta, S., Song, Z., Li, K., Arora, S., 2021. Evaluating gradient inversion attacks and defenses in federated learning. Advances in Neural Information Processing Systems 34, 7232–7241.
- Jin, R., Li, X., 2022. Backdoor attack is a devil in federated gan-based medical image synthesis, in: International Workshop on Simulation and Synthesis in Medical Imaging, Springer. pp. 154–165.
- Karras, T., Aittala, M., Hellsten, J., Laine, S., Lehtinen, J., Aila, T., 2020. Training generative adversarial networks with limited data. Advances in Neural Information Processing Systems 33, 12104–12114.
- Kermany, D.S., Goldbaum, M., Cai, W., Valentim, C.C., Liang, H., Baxter, S.L., McKeown, A., Yang, G., Wu, X., Yan, F., et al., 2018. Identifying medical diagnoses and treatable diseases by image-based deep learning. Cell 172, 1122–1131.
- Kirkpatrick, J., Pascanu, R., Rabinowitz, N., Veness, J., Desjardins, G., Rusu, A.A., Milan, K., Quan, J., Ramalho, T., Grabska-Barwinska, A., et al., 2017. Overcoming catastrophic forgetting in neural networks. Proceedings of the national academy of sciences 114, 3521–3526.
- Kolouri, S., Saha, A., Pirsiavash, H., Hoffmann, H., 2020. Universal litmus patterns: Revealing backdoor attacks in cnns, in: Proceedings of the IEEE/CVF Conference on Computer Vision and Pattern Recognition, pp. 301–310.
- Konečný, J., McMahan, H.B., Yu, F.X., Richtárik, P., Suresh, A.T., Bacon, D., 2016. Federated learning: Strategies for improving communication efficiency. arXiv preprint arXiv:1610.05492 .
- Li, Y., Jiang, Y., Li, Z., Xia, S.T., 2022. Backdoor learning: A survey. IEEE Transactions on Neural Networks and Learning Systems .
- Li, Y., Lyu, X., Koren, N., Lyu, L., Li, B., Ma, X., 2021a. Anti-backdoor learning: Training clean models on poisoned data. Advances in Neural Information Processing Systems 34, 14900–14912.
- Li, Y., Zhai, T., Jiang, Y., Li, Z., Xia, S.T., 2021b. Backdoor attack in the physical world. arXiv preprint arXiv:2104.02361 .
- Li, Y., Zhai, T., Wu, B., Jiang, Y., Li, Z., Xia, S., 2020. Rethinking the trigger of backdoor attack. arXiv preprint arXiv:2004.04692 .
- Lin, Y., Wang, Z., Cheng, K.T., Chen, H., 2022. Insmix: Towards realistic generative data augmentation for nuclei instance segmentation. arXiv preprint arXiv:2206.15134 .
- Liu, F.T., Ting, K.M., Zhou, Z.H., 2008. Isolation forest, in: 2008 eighth IEEE international conference on data mining, IEEE. pp. 413–422.
- Liu, X., Li, W., Yuan, Y., 2022. Intervention & interaction federated abnormality detection with noisy clients, in: International Conference on Medical Image Computing and Computer-Assisted Intervention, Springer. pp. 309–319.
- Liu, Y., Ma, X., Bailey, J., Lu, F., 2020. Reflection backdoor: A natural backdoor attack on deep neural networks, in: European Conference on Computer Vision, Springer. pp. 182–199.
- Liu, Y., Xie, Y., Srivastava, A., 2017. Neural trojans, in: 2017 IEEE International Conference on Computer Design (ICCD), IEEE. pp. 45–48.
- Malin, B.A., Emam, K.E., O’Keefe, C.M., 2013. Biomedical data privacy: problems, perspectives, and recent advances. Journal of the American medical informatics association 20, 2–6.
- McMahan, B., Moore, E., Ramage, D., Hampson, S., y Arcas, B.A., 2017. Communication-efficient learning of deep networks from decentralized data, in: Artificial intelligence and statistics, PMLR. pp. 1273–1282.
- Mirza, M., Osindero, S., 2014. Conditional generative adversarial nets. arXiv preprint arXiv:1411.1784 .
- Nelson, B., Barreno, M., Chi, F.J., Joseph, A.D., Rubinstein, B.I., Saini, U., Sutton, C., Tygar, J.D., Xia, K., 2008. Exploiting machine learning to subvert your spam filter. LEET 8, 9.
- Ozdayi, M.S., Kantarcioglu, M., Gel, Y.R., 2021. Defending against backdoors in federated learning with robust learning rate, in: Proceedings of the AAAI Conference on Artificial Intelligence, pp. 9268–9276.
- Pillutla, K., Kakade, S.M., Harchaoui, Z., 2019. Robust aggregation for federated learning. arXiv preprint arXiv:1912.13445 .
- Pogorelov, K., Randel, K.R., Griwodz, C., Eskeland, S.L., de Lange, T., Johansen, D., Spampinato, C., Dang-Nguyen, D.T., Lux, M., Schmidt, P.T., et al., 2017. Kvasir: A multi-class image dataset for computer aided gas-

- triointestinal disease detection, in: Proceedings of the 8th ACM on Multimedia Systems Conference, pp. 164–169.
- Price, W.N., Cohen, I.G., 2019. Privacy in the age of medical big data. *Nature medicine* 25, 37–43.
- Qiu, H., Zeng, Y., Guo, S., Zhang, T., Qiu, M., Thuraisingham, B., 2021. Deep-sweep: An evaluation framework for mitigating dnn backdoor attacks using data augmentation, in: Proceedings of the 2021 ACM Asia Conference on Computer and Communications Security, pp. 363–377.
- Radford, A., Metz, L., Chintala, S., 2015. Unsupervised representation learning with deep convolutional generative adversarial networks. *arXiv preprint arXiv:1511.06434*.
- Rasouli, M., Sun, T., Rajagopal, R., 2020. Fedgan: Federated generative adversarial networks for distributed data. *arXiv preprint arXiv:2006.07228*.
- Rawat, A., Levacher, K., Sinn, M., 2021. The devil is in the gan: Defending deep generative models against backdoor attacks. *arXiv preprint arXiv:2108.01644*.
- Rieke, N., Hancox, J., Li, W., Milletari, F., Roth, H.R., Albarqouni, S., Bakas, S., Galtier, M.N., Landman, B.A., Maier-Hein, K., et al., 2020. The future of digital health with federated learning. *NPJ digital medicine* 3, 1–7.
- Saha, A., Subramanya, A., Pirsiavash, H., 2020. Hidden trigger backdoor attacks, in: Proceedings of the AAAI conference on artificial intelligence, pp. 11957–11965.
- Salem, A., Sautter, Y., Backes, M., Humbert, M., Zhang, Y., 2020. Baan: Backdoor attacks against autoencoder and gan-based machine learning models. *arXiv preprint arXiv:2010.03007*.
- Scherer, J., Nolden, M., Kleesiek, J., Metzger, J., Kades, K., Schneider, V., Bach, M., Sedlaczek, O., Bucher, A.M., Vogl, T.J., et al., 2020. Joint imaging platform for federated clinical data analytics. *JCO clinical cancer informatics* 4, 1027–1038.
- Shorten, C., Khoshgoftaar, T.M., 2019. A survey on image data augmentation for deep learning. *Journal of big data* 6, 1–48.
- Song, Y., Sohl-Dickstein, J., Kingma, D.P., Kumar, A., Ermon, S., Poole, B., 2021. Score-based generative modeling through stochastic differential equations. *The International Conference on Learning Representations*.
- Sun, G., Cong, Y., Dong, J., Wang, Q., Lyu, L., Liu, J., 2021. Data poisoning attacks on federated machine learning. *IEEE Internet of Things Journal* 9, 11365–11375.
- Sun, Z., Kairouz, P., Suresh, A.T., McMahan, H.B., 2019. Can you really backdoor federated learning? *arXiv preprint arXiv:1911.07963*.
- Teramoto, A., Tsukamoto, T., Yamada, A., Kiriya, Y., Imaizumi, K., Saito, K., Fujita, H., 2020. Deep learning approach to classification of lung cytological images: Two-step training using actual and synthesized images by progressive growing of generative adversarial networks. *PloS one* 15, e0229951.
- Tolpegin, V., Truex, S., Gursoy, M.E., Liu, L., 2020. Data poisoning attacks against federated learning systems, in: Computer Security–ESORICS 2020: 25th European Symposium on Research in Computer Security, ESORICS 2020, Guildford, UK, September 14–18, 2020, Proceedings, Part I 25, Springer, pp. 480–501.
- Usynin, D., Klause, H., Paetzold, J.C., Rueckert, D., Kaissis, G., 2022. Can collaborative learning be private, robust and scalable?, in: International Workshop on Distributed, Collaborative, and Federated Learning, Workshop on Affordable Healthcare and AI for Resource Diverse Global Health, Springer, pp. 37–46.
- Van Panhuis, W.G., Paul, P., Emerson, C., Grefenstette, J., Wilder, R., Herbst, A.J., Heymann, D., Burke, D.S., 2014. A systematic review of barriers to data sharing in public health. *BMC public health* 14, 1–9.
- Villarreal-Vasquez, M., Bhargava, B., 2020. Confoc: Content-focus protection against trojan attacks on neural networks. *arXiv preprint arXiv:2007.00711*.
- Wang, B., Yao, Y., Shan, S., Li, H., Viswanath, B., Zheng, H., Zhao, B.Y., 2019. Neural cleanse: Identifying and mitigating backdoor attacks in neural networks, in: 2019 IEEE Symposium on Security and Privacy (SP), IEEE, pp. 707–723.
- Wang, H., Sreenivasan, K., Rajput, S., Vishwakarma, H., Agarwal, S., Sohn, J.y., Lee, K., Papailiopoulos, D., 2020a. Attack of the tails: Yes, you really can backdoor federated learning. *Advances in Neural Information Processing Systems* 33, 16070–16084.
- Wang, H., Yurochkin, M., Sun, Y., Papailiopoulos, D., Khazaeni, Y., 2020b. Federated learning with matched averaging. *arXiv preprint arXiv:2002.06440*.
- Wang, Z., Chen, J., Hoi, S.C., 2020c. Deep learning for image super-resolution: A survey. *IEEE transactions on pattern analysis and machine intelligence* 43, 3365–3387.
- Woodland, M., Wood, J., Anderson, B.M., Kundu, S., Lin, E., Koay, E., Odisio, B., Chung, C., Kang, H.C., Venkatesan, A.M., et al., 2022. Evaluating the performance of stylegan2-ada on medical images, in: International Workshop on Simulation and Synthesis in Medical Imaging, Springer, pp. 142–153.
- Xu, X., Wang, Q., Li, H., Borisov, N., Gunter, C.A., Li, B., 2021. Detecting ai trojans using meta neural analysis, in: 2021 IEEE Symposium on Security and Privacy (SP), IEEE, pp. 103–120.
- Xue, C., Yu, L., Chen, P., Dou, Q., Heng, P.A., 2022. Robust medical image classification from noisy labeled data with global and local representation guided co-training. *IEEE Transactions on Medical Imaging* 41, 1371–1382.
- Ying, Z., Zhang, Y., Liu, X., 2020. Privacy-preserving in defending against membership inference attacks, in: Proceedings of the 2020 Workshop on Privacy-Preserving Machine Learning in Practice, pp. 61–63.
- Yu, S., Zhang, S., Wang, B., Dun, H., Xu, L., Huang, X., Shi, E., Feng, X., 2021. Generative adversarial network based data augmentation to improve cervical cell classification model. *Math. Biosci. Eng* 18, 1740–1752.
- Zeng, Y., Chen, S., Park, W., Mao, Z.M., Jin, M., Jia, R., 2021a. Adversarial unlearning of backdoors via implicit hypergradient. *arXiv preprint arXiv:2110.03735*.
- Zeng, Y., Park, W., Mao, Z.M., Jia, R., 2021b. Rethinking the backdoor attacks’ triggers: A frequency perspective, in: Proceedings of the IEEE/CVF International Conference on Computer Vision, pp. 16473–16481.
- Zhang, K., Tao, G., Xu, Q., Cheng, S., An, S., Liu, Y., Feng, S., Shen, G., Chen, P.Y., Ma, S., et al., 2022. Flip: A provable defense framework for backdoor mitigation in federated learning. *arXiv preprint arXiv:2210.12873*.
- Zhang, R., Isola, P., Efros, A.A., Shechtman, E., Wang, O., 2018. The unreasonable effectiveness of deep features as a perceptual metric, in: Proceedings of the IEEE conference on computer vision and pattern recognition, pp. 586–595.
- Zheng, S., Zhang, Y., Wagner, H., Goswami, M., Chen, C., 2021. Topological detection of trojaned neural networks. *Advances in Neural Information Processing Systems* 34, 17258–17272.
- Zhu, C., Zhang, J., Sun, X., Chen, B., Meng, W., 2023. Adfl: Defending backdoor attacks in federated learning via adversarial distillation. *Computers & Security*, 103366.
- Zhu, L., Ning, R., Wang, C., Xin, C., Wu, H., 2020. Gangsweep: Sweep out neural backdoors by gan, in: Proceedings of the 28th ACM International Conference on Multimedia, pp. 3173–3181.